Improving fiber orientation estimation in constrained spherical deconvolution under non-white matter partial volume effects

Timo Roine[1], Ben Jeurissen[1], Wilfried Philips[2], Alexander Leemans[3], and Jan Sijbers[1]

[1]*iMinds-Vision Lab, University of Antwerp, Antwerp, Flanders, Belgium,* [2]*Department of Telecommunications and Information Processing, University of Ghent, Ghent, Flanders, Belgium,* [3]*Image Sciences Institute, University Medical Center Utrecht, Utrecht, Netherlands*

Purpose: In this study, we investigated partial volume effects (PVEs) of non-white matter (WM) tissue in constrained spherical deconvolution (CSD) [1]. Diffusion-weighted (DW) magnetic resonance imaging (MRI) is prone to significant PVEs due to its limitations in spatial resolution [2]. While able to detect multiple crossing or kissing fiber configurations, non-WM PVEs are not adequately addressed in CSD. We performed simulations to study these non-WM PVEs, and based on the results, we propose a modification to CSD to further improve the estimation of the fiber orientation distribution function (fODF).

Methods: In CSD, the fODF is deconvolved from the DW signal using a kernel that represents the DW signal corresponding to a single fiber orientation (i.e. the response function, RF). During this deconvolution procedure, the negative peaks are suppressed to reliably solve the ill-posed and noise-sensitive deconvolution problem [3-4]. The RF is the DW signal of an ideal fiber population perfectly aligned along the z-axis, and can be estimated from real data by a recursive calibration [5] or by selecting voxels with high fractional anisotropy, aligning their principal eigenvectors along the z-axis and averaging their spherical harmonics (SH) decompositions. We propose a modification to CSD, in which non-WM signal is included in the RF when non-WM PVEs are present. In the simulations, this equals to adding an appropriate fraction of simulated gray matter (GM), cerebrospinal fluid (CSF), or air signal into the simulated noisy RF. In practice, the signal in GM and CSF can be estimated from real DW data, and the fraction of non-WM tissue in a voxel based on high-resolution structural MRI data.

Newton optimization was used to extract the peaks of the fODF directly based on the SH decompositions [6]. Measures for accuracy (bias) and precision (95 % confidence interval, CI), and the number of true and false fiber orientations were calculated by clustering the peaks and using a mean dyadic tensor [7]. Peaks were accepted if they were less than 35 degrees from the mean dyadic tensor and larger than 33 % of the maximum amplitude of the fODF.

Simulations were performed to compare the results to the original version of CSD. We simulated GM and WM tissue with a mean diffusivity of 0.0007 mm^2/s, CSF tissue with 0.002 mm^2/s [8], and in air, signal was assumed to be zero. The angle between two crossing fiber populations was set at 70 degrees, diffusion weighting was 3000 s/mm^2 and up to 8^{th} order spherical harmonics were used. SNR was 30, and different noise realizations were used to simulate 1000 iterations for each isotropic volume fraction using a different gradient set in each of the iterations to prevent an orientation bias.

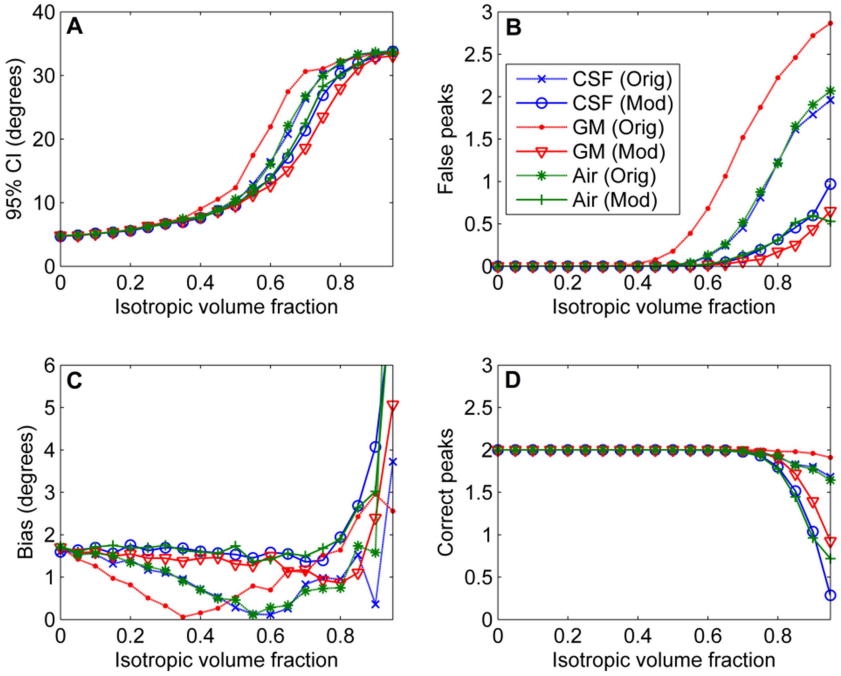

Fig. 1: Non-WM PVEs in CSD (Orig) and with the proposed modification (Mod), using up to 8^{th} order SH, diffusion weighting 3000 s/mm^2, angle 70° and SNR 30.

Results: The precision of the detected fiber orientations decreased and a high number of false peaks emerged when the isotropic non-WM tissue fraction increased (Fig. A & B). The effect was stronger in the case of gray matter (GM) tissue, and remained significant even when the SNR increased. In the case of CSF, the effects were similar to air partial volume. The proposed modification significantly improved the precision and decreased the number of false peaks detected (Fig. A & B). Accuracy of the peaks was not affected (Fig. C).

Discussion: Our results show that the fODF estimation in CSD is highly sensitive to GM PVEs. Part of the effects is caused by the decrease in WM fraction and part by the isotropic signal from GM tissue. Non-WM PVEs can hinder the propagation of tracts entering the cortical GM or passing close to sub-cortical GM, which has severe implications in tractography. Similar problems are present with CSF tissue, but are largely caused by the decreased WM fraction, which affects the SNR, as shown by the comparison to air volume. The proposed method significantly improves precision and the number of false peaks found, but caused a small loss in angular resolution with very high isotropic fractions (Fig. D). However, with the proposed method the true peaks were found with better precision up to isotropic fractions of 0.6-0.8, while the number of false peaks remained very low.

Methods to discard tracts based on their anatomical feasibility already exist [9]. However, it would be more efficient and more accurate to correct for the PVEs before tractography for example with the method proposed here. This would enable tracts to proceed directly into the cortical GM or pass close to subcortical GM, which would in turn significantly reduce the tracking time, and minimize any bias in the end points of the tracts caused by the random distribution of WM fraction in the voxels in the WM-GM interface.

Conclusion: We showed that the precision of the detected fiber orientations decreased and false peaks emerged in voxels with non-WM PVEs, which was more prominently expressed with GM tissue. The proposed method significantly improved the results, and would be beneficial for tractography in areas where tracts enter or pass GM tissue.

References: [1] Tournier, J. et al. (2007). NeuroImage, 35(4), 1459-1472. [2] Jones, D. K. & Cercignani, M. (2010). NMR in Biomed, 23(7), 803-820. [3] Tournier, J. et al. (2004). NeuroImage, 23(3), 1176-1185. [4] Tournier, J. et al. (2008). Neuroimage, 42(2), 617-625. [5] Tax, C. M. V. et al. (2013). NeuroImage, in press. [6] Jeurissen, B. et al. (2013). Hum Brain Mapp, 34(11), 2747-2766. [7] Jones, D. K. (2003). Magnet Reson Med 49:7–12. [8] Dell'Acqua, F. et al. (2010). Neuroimage, 49(2), 1446-1458. [9] Smith, R. E. et al. (2012). NeuroImage, 62(3), 1924-1938.